ELSEVIER

IMAVIS 1084T

Image and Vision Computing 14 (1996) 741–752

image and vision COMPUTING

Median-type filters with model-based preselection masks

Lina García-Cabrera[a], M. José García-Salinas[b], Pedro L. Luque-Escamilla[c], José Martínez-Aroza[d], Juan F. Gómez Lopera[b], Ramón Román-Roldán[c,*]

[a]*Departamento de Informática, Universidad de Jaén, Spain*
[b]*Departamento de Física Aplicada, Universidad de Almería, Spain*
[c]*Departamento de Física Aplicada, Universidad de Granada, Avda. Fuente Nueva, s/n 18.071 Granada, Spain*
[d]*Departamento de Matemática Aplicada, Universidad de Granada, Spain*

Received 10 February 1995; revised 11 January 1996

Abstract

To remove impulsive noise, several variants of median-type filters are presented. They use some prior information provided by the probabilistic composition model of the class of the image being processed. This information is doubly applied; first, in elaborating a noise-estimation mask for the preselection of the pixels which must be filtered; and second, in the filtering process itself. The aim is to avoid the side-effect damage that median-type filters produce in processing the non-contaminated pixels. Experimental results are better than in the conventional median filter.

Keywords: Median filter; Noisy pixels detection; Composition matrix; Prefiltering mask

1. Introduction

Within the spatial non-linear filters, order statistic filters are receiving increasing attention, mainly because of their efficiency in removing impulsive noise [1]. The theoretical basis for their study is the Robust-Statistics Theory [2], thus these filter show the outstanding property of robustness, as given by the breakpoint.

Among the wide variety of statistic filters, the simple median filter (see Refs. [3,4] and references therein) occupies a prominent place, due to its computational simplicity, its robustness and its thresholding property, which allows this filter to be included in the stack-filter category [5]. A broad theoretical study has been made, particularly with respect to the roots, that is to say, the images that remain invariant in the filtering.

The most distinguished feature of the median filters is their ability to remove the impulsive noise while preserving the edges in the image. To improve this performance, a number of modified median filters have been developed, like the separable median filter, the mean α-trimmed filter, the max/med filters and the L-filters.

In this paper new median-type filters, called Mask-Model Filters, are introduced. The starting point is that a spatial filter damages some good pixels by itself, and this must be avoided. This problem is addressed by:

1. The use of some prior information by means of the probabilistic composition model for the class of images worked on [6]. This is a stochastic model revealing the typical histogram of a window in any image of the class. It is referred to as the model or the composition matrix.
2. The selection of the subset of noisy pixels which must be filtered, the others being unaltered [7]. This selection is performed before the filtering process, by preparing a mask with the pixels estimated as corrupted, according to the information provided by the composition matrix. The mask is referred to as the noise-estimation mask (NEM). Both concepts are studied in the following section.

As derived from the general class of median filters, the Mask-Model filters are in the same category and have the same field of application: they provide enhancement processes for removing impulsive noise. However, resorting to some information related to the image somewhat approximates the enhancement process to a restoration

* Corresponding author.

0262-8856/96/$15.00 © 1996 Elsevier Science B.V. All rights reserved
PII S0262-8856(96)01084-0

one. This is more pronounced in the fourth filter presented, the model-restoration filter, in which the criterion of maximum closeness to the class is used.

2. Operational features

2.1. Basics

Impulsive noise affects only a fraction of the pixels in an image. Thus, an original image O is affected by impulsive noise in this way:

$$S = OM + N(1 - M)$$

where N is a noise-image coming from an i.i.d. source of noise, M is a mask indicating which pixels are to be changed, and S, the noisy image, is the input of any filter. All images appearing in this expression are of the same size, and arithmetic operations between them are performed pixel by pixel. The filtering process $S \rightarrow R \approx O$ gives as a result an image R as close as possible to the original.

The four filters proposed here are based on two concepts: (1) the preselection mask (NEM) to reduce the processing to the pixels estimated as corrupted; (2) the composition matrix, which provides some information about the image. Both are discussed below for self-contained work.

2.2. Composition models

In our approach, each image belongs to a class $\mathscr{C}$ (radiographs, echographs, ...) represented by a composition matrix [6]. This is a bidimensional array describing the histograms provided by a sliding window covering all images in the class. By defining the window grey level k' as the sum of grey levels of the pixels in the window, every column $Q_{k'}$ in the composition matrix is the average histogram of all windows with the same k'. There are as many columns as window grey levels, i.e. from 0 to $G \cdot w$, where G is the maximum grey level of the pixels, and w is the size of the window:

$$Q(\mathscr{C}) = (Q_0 Q_1 \ldots Q_{Gw}).$$

Thus, the kth element in $Q_{k'}$ is the relative frequency of grey level k for pixels inside sliding windows with grey level k'. If there were no windows with grey level k' then $Q_{k'}$ could not be calculated. In this case, we should consider that the grey level k' does not exist in $\mathscr{C}$, and the composition matrix would have an empty column in $Q_{k'}$.

It is obvious that we cannot handle all the images of the same class. However, a composition matrix can be obtained in two ways: first, by theoretical means, formulating hypotheses about the internal structure of the regions [8], for example, the hypergeometrical model: second, by empirical means, computing the matrix columns $Q_{k'}$ by averaging the histograms of all the regions in a selected sample, from an appropriate set of images of the same class $\mathscr{C}$. By doing the same for each k', the matrix $Q(\mathscr{C})$ is obtained [9]. This estimated composition model may be used for filtering any image belonging to the class it represents.

When the composition model is applied for either constructing the preselection mask or filtering, a prediction about the grey level k of a pixel is made. The reliability of this prediction depends on the quality of the composition model, which in turn relies on the sample size and on the compositional homogeneity of the windows in the sample. This homogeneity should be specified in terms of some appropriate measure of cohesion between the histograms (i.e. probability distributions) of the observed windows in the training sample. For this purpose we use the Jensen–Shannon divergence (JS) [10] for each column $Q_{k'}$ in the composition model:

$$JS(Q_{k'}) = H(Q_{k'}) - \frac{1}{N_{k'}} \sum_{i=1}^{N_{k'}} H(\mathscr{P}_i)$$

where every $\mathscr{P}_i$ stands for the histogram obtained from a window with grey level k'; and $H(\cdot) = \Sigma p \log p$ is the Shannon entropy of the argument probability distribution. For our purposes, here it suffices to bear in mind that the lower JS is, the more cohesion the sample has, the better defined is the class of images, and the better the composition model $Q(\mathscr{C})$ should behave. A more detailed description of the usage of JS to qualify classes of images is given in Ref. [9].

2.3. The noise-estimation mask (NEM)

We now have information about the probability of finding a grey level k inside a region with window grey-level k'; therefore, it may be decided whether or not a certain grey level is noisy. We define *selection* as the process of deciding whether a pixel has a likely grey level, according to the composition matrix. This selection is determined by means of the choice of a threshold κ^* in the ordered histogram of the column $Q_{k'}$, $(Q_{k'})_{[\cdot]}$. Every grey level k verifying $(Q_{k'})_{[k]} > (Q_{k'})_{[\kappa^*]}$ is considered to be probable, and thus the corresponding pixel is not filtered. This threshold can be characterized by a certain selection ratio $\rho \in [0, 1]$, as follows: given ρ, then a unique κ^* exists, such that

$$\sum_{\kappa=0}^{\kappa^*} (Q_{k'})_{[\kappa]} \leq \rho < \sum_{\kappa=0}^{\kappa^*+1} (Q_{k'})_{[\kappa]},$$

and thus the grey levels $[0], [1], \ldots, [k^*]$ will be considered as noisy if they are found in windows with grey level k'. This selected subset of grey levels is better determined in practice by having constructed the ordered column $(Q_{k'})_{[\kappa]}$ beforehand in a look-up-table fashion. Thus, the entry of this look-up table (LUT) is the window

grey level k', and the output is the set of grey levels not to be filtered.

Extreme values for ρ means: (1) $0 \leq \rho < (Q_{k'})_{[0]}$, no pixels are to be filtered; (2) $\rho = \Sigma(Q_{k'}) = 1$, all pixels are to be filtered (no selection at all). The full theoretical analyses of the parameter ρ in relation to the filter performance seems to be quite untractable. While some approach is in progress, heuristic settings should be made.

Since the window grey level is altered by noise in the source image, then the use of the LUT is somewhat wrong. This can be avoided by implementing an iterative procedure that shows good convergence properties. More details about the construction of the NEM are not needed here, and will be found in future work [7].

Despite the building process itself for the NEM, its quality should be considered. Two measures of quality are defined next, which represent the degree of success in the noise estimation in the image. They are the proportions of good and bad pixels found with no error:

detection ratio in *defined by*

undamaged pixel, $\text{udr} = \Sigma(M\tilde{M})/\Sigma(M)$

damaged pixel, $\text{ddr} = \Sigma[(1-M)(1-\tilde{M})]/\Sigma(1-M)$,

where $\tilde{M}$ is the NEM and M is the real mask. Notice that ddr is more relevant than udr, since an error in respect to the first means that a noisy pixel will not be filtered, but in the second it means that a good pixel will be. Numerical values of ddr and udr are usually above 95% after 5, 6 iterations, as can be seen in the given examples. The measures are next used to show the influence of the composition matrix and the selection ratio on the quality of the mask.

2.4. Influence of the quality of the composition matrix on the mask

The composition matrix $Q(\mathscr{C})$ plays an important role in the construction of the NEM. It is expected that the better the quality of $Q(\mathscr{C})$, the more adjusted the NEM is, as given by its udr and ddr values. This behavior is shown in Table 1. The NEM is built from a source image with 20% uniformly distributed impulsive noise and a selection ratio of 0% (the reason for this is discussed later). The quality of $Q(\mathscr{C})$ is evaluated by means of the JS divergence measure. It is apparent that when the divergence measure is lower, the NEM obtained is better adjusted.

Table 1
Experimental results showing the influence of the model quality on the mask fitness

	JS	udr	ddr	window size
Q(text)	1.65	99.28	49.76	3 × 3
Q(eco)	0.75	100.00	79.82	3 × 3
Q(rad)	0.03	96.91	96.68	3 × 3
Q(text)	0.80	99.93	46.59	5 × 5
Q(eco)	0.48	99.97	77.54	5 × 5
Q(rad)	0.05	96.72	96.58	5 × 5

Table 2
A strange model leads to a wrong mask

	udr	ddr
$Q(\mathscr{C} = \textit{radiograph})$	90.62	95.77
$Q(\mathscr{C}' = \textit{echograph})$	51.78	75.23

The influence of the model on the quality of $\tilde{M}$ may be studied from another point of view. By using the model of another class $Q(\mathscr{C}')$, a different NEM $\tilde{M}'$ is obtained from the same source image S. It is expected that $\tilde{M}$ was much better than $\tilde{M}'$, because of the adequacy between S and $Q(\mathscr{C})$. This is illustrated in Table 2, where the source S is a radiograph corrupted with 30% uniformly distributed impulsive noise, and the size of the window is 5 × 5.

2.5. Influence of the selection ratio on the mask

Another feature that may determine the reliability of the NEM is the selection ratio, ρ. If it has small values, only pixels whose grey level has a low probability will be taken as bad ones. As ρ grows, more pixels are chosen as noisy. Thus, the quality of the NEM may be improved by suitably changing the value of the selection ratio, as can be seen in Table 3. This was made from a text source image with 20% uniformly distributed impulsive noise, and 5 × 5 window size.

Making a note on the choosing of the selection ratio ρ is worthwhile. When estimating the window grey level, an error is introduced due to the noise, and then a wrong (but fairly close) entry of the LUT is consulted; thus, the decision about which pixels are good or bad is somewhat altered. If a low value for ρ is set, then all the pixels marked as bad will have a very small probability according to the wrong entry of the LUT, so they probably will still be bad according to entries in a neighbourhood. As a consequence, a low value for ρ makes the marking of bad pixels robust against noise. Perhaps the convergence of the mask is slower, but it is preferable because the growing quality of successive iterations is guaranteed.

Table 3
Influence of the selection ratio

ρ (%)	udr	ddr
0	99.93	46.55
1	99.54	61.41
2	98.85	67.96

Original

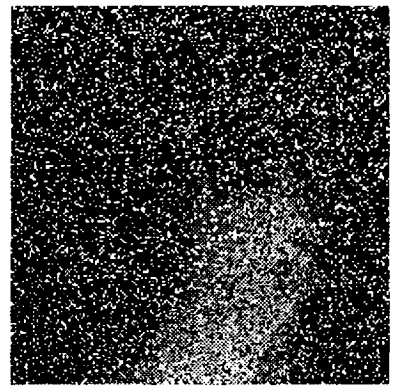

Source
(30 % salt & pepper noise)

5 × 5 Median Filter

5 × 5 Central Weighted Median Filter

Adaptive Filter
(Sun & Venetsanopoulos)

5 × 5 Mask-Median Filter
(selection ratio $\rho = 0\%$)

Fig. 1. Median and central weighted median filtering, Sun & Venetsanopoulos' adaptive filtering and mask-median filtering example for a radiograph image. (a) Original, (b) source (30% salt & pepper noise), (c) 5 × 5 Median filter, (d) 5 × 5 Central Weighted Median filter, (e) Adaptive filter (Sun & Venetsanopoulos), (f) 5 × 5 Mask-Median filter (selection ratio $\rho = 0\%$).

3. Filters

Four Mask-Model filters are described next. The first three calculate the median of: (1) the window; (2) the model; (3) the window weighted by the model. The fourth uses the max operator on a probabilistic model-belonging table. For each filter, an example is carried out with an image belonging to a known class $Q(\mathscr{C})$; except of that for the Model Restoration filter, which uses a theoretical model based on the hypergeometric distribution. The results are shown visually, and compared with those obtained from the well-known conventional median, central weighted median and adaptive (Sun & Venetsanopoulos) [11] filters. Numerical results are given at large.

The reasons for choosing that filters for comparison are the following. First, one of them is a nonadaptive filter, having the advantage of not requiring prior information about the image, nor needing to compute local statistics inside the (fixed) window, leading to a faster and simpler algorithm. The other is an adaptive one, with a fixed window, that needs to calculate expectation and variance inside to estimate noise and then to get the minimum mean square error result. Thus the proposed filters can be compared with well-known filters that improve the median, one of them using prior information like ours. Other kinds of filter, like FIR-Hybrid or Multistage-Median, have been rejected in our comparison, because they preserve noise structures instead of attenuating them when impulsive noise is high (20%, 30%) [12,13]. The Multistage-Median also has breakdown probabilities greater than the conventional median, so it performs worse than the latter when noise is high. Therefore, our filters work much better than the Multistage-Median, as is verified, because they are better than the conventional median in noise attenuation and detail preserving.

As regards the kind of noise used in our experiments, it should be noticed that only impulsive noise (salt & pepper and uniformly distributed) has been studied. This is because the Gaussian noise affects all pixels in the image, that is, all the pixels are noisy. Therefore, the NEM cannot be properly calculated, and the results of filtering are thus erroneous. Only impulsive noise, affecting the image partially, can be used for building a NEM with good performance.

3.1. Mask-median filter

Operation. This simple filter is the conventional median filter operating with the preselection mask. The model $Q(\mathscr{C})$ is used here only for building the NEM, and not in the filtering process. The working operation is easy: for each position (i,j) marked as bad ($\tilde{M}_{i,j}=0$), the median of the centered window W_{ij} is computed.

This filter is described as:

$$R_{ij} - S_{ij}\,\tilde{M}_{ij} + \text{med}(W_{ij}(S))(1-\tilde{M}_{ij}).$$

As an example, a radiograph image corrupted by 30% of salt & pepper noise is filtered. The results are shown in Fig. 1, using the parameters as indicated. While noise is well removed by all filters, the original is better preserved by the Mask-Median filter.

3.2. Mask-matrix filter

Operation. This filter substitutes the corrupted grey level by the median, not of the window, but of the appropriate $Q_{k'}$. Since this is a probability distribution, its median is the grey level of the accumulated probability 0.5. The filtering steps are:

1. **Window grey level estimation**. For each proper window position, (i,j) such as $\tilde{M}_{i,j}=0$ the partial window grey level $\Sigma[(W_{ij}(S\tilde{M})]$ is computed as the sum of the grey level of all the mask-good pixels included. Then, the total window grey level is estimated as that of a noise-clear window with the same average grey level:

$$k' = \tilde{\Sigma}[W_{ij}(S),\tilde{M}] = \Sigma[W_{ij}(S\tilde{M})]\frac{(2v_w+1)\times(2h_w+1)}{\Sigma[W_{ij}(\tilde{M})]}. \quad (1)$$

2. **The median of the matrix column.** The matrix $Q(\mathscr{C})$ provides the probability distribution for k. The median of the column k' is taken, given an estimate: $k_e = \text{med}(Q_{k'})$.

The filter operation with the median is described as

$$R_{ij} = S_{ij}\tilde{M}_{ij} + \text{med}(Q_{k'})(1-\tilde{M}_{ij}),$$

where k' is obtained in (1)

Comparative results of filtering a text image with 10% uniform noise are given in Fig. 2. The best performance is obtained by the Mask-Matrix filter. The original detail preservation and the absence of blotches in the background is easily observed.

3.3. Mask-model weighted filter

Operation. As a refinement of the above, this filter also takes into account the histogram of the window and weighs it with the matrix column. It operates as follows: the window histogram $\mathscr{P}[W_{ij}(S\tilde{M})]$ is weighed by the column distribution $W_{k'}, k'$ obtained as in Eq. (1), giving the $(G+1)$ vector

$$\mathscr{P}^*(\mathscr{P},Q_{k'}) = \mathscr{P}[W_{ij}(S\tilde{M})]\cdot Q_{k'},$$

and the median of the weighted window histogram is taken.

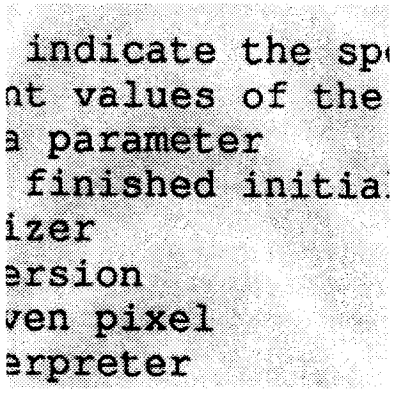

Original

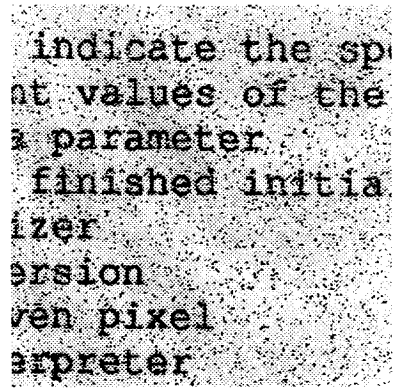

Source
(10% uniformly distributed noise)

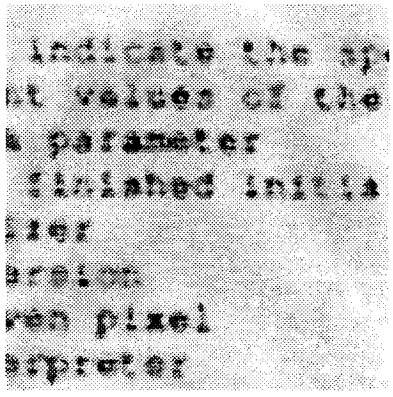

5×5 Median Filter

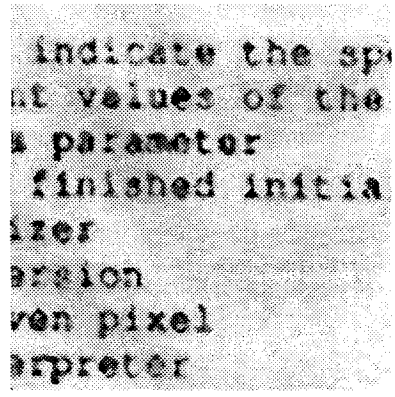

5×5 Central Weighted Median Filter

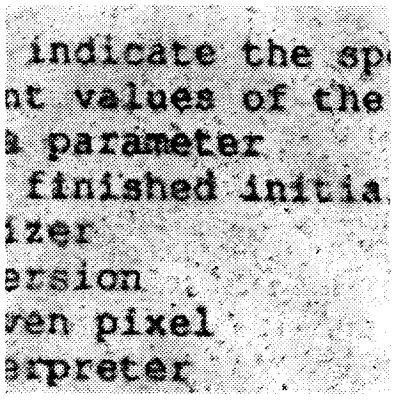

Adaptive Filter
(Sun & Venetsanopoulos)

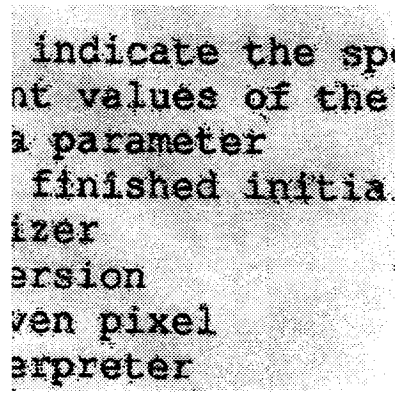

5×5 Mask-Matrix Filter
(selection ratio $\rho = 1\%$)

Fig. 2. Median and center weighted median filtering, Sun & Venetsanopoulos adaptive filtering and mask-matrix filtering example for a text image. (a) Original, (b) source (10% uniformly distributed noise), (c) 5 × 5 Median filter, (d) 5 × 5 Central Weighted Median filter, (e) Adaptive filter (Sun & Venetsanopoulos), (f) 5 × 5 Mask-Matrix filter (selection ratio $\rho = 1\%$).

The operation of this filter is

$$R_{ij} = S_{ij}\tilde{M}_{ij} + \text{med}(\mathscr{P}^*)(1 - \tilde{M}_{ij}).$$

As an example, an echograph image affected by 20% uniform noise is filtered. Comparative results are given in Fig. 3, with parameters as indicated. The noise is better removed by the Mask-Model Weighted filter than by the reference filters. Details are also better preserved.

3.4. Model-restoration filter

Operation. In this more elaborate procedure, a criterion of closeness of the filtered image to its model is implemented. The final grey level of the processed pixel is taken to maximize the probability for the window to resemble the model. The operation steps for this filter are:

1. **Window grey level estimation**. This is the same as step 1 of the mask-median filter, but this time a quasi-total grey level is estimated, for a reduced window of size $(2v_w + 1) \times (2h_w + 1) - 1$:
$$k'_0 = \Sigma[W_{ij}(S\tilde{M})]\frac{(2v_w + 1) \times (2h_w + 1) - 1}{\Sigma[W_{ij}(\tilde{M})]}.$$
2. **k-testing**. Adding each possible grey level $k = 0, 1, 2, \ldots, G$ of the central pixel to the above estimated grey level, produces the corresponding window grey level, $k' = k'_0 + k$ (this would have been obtained if k had been correct).
3. **Diagonal probabilities**. For each k, the probability of containing the tested grey level k is computed from the corresponding $Q_{k'_0+k}$. This set of probabilities is placed in a diagonal of Q with heading k'_0. These do not constitute a distribution, since they all belong to different columns.
4. **Maximum**. From all the probabilities in the diagonal, the maximum is determined, its grey level k^* being the filtering result.

This filter operation is described as:

$$R_{ij} = S_{ij}\tilde{M}_{ij} + k^*(1 - \tilde{M}_{ij}),$$
$$\text{where } (Q_{k'_0+k^*})_{k^*} \geq (Q_{k'_0+k})_k \quad \forall k = 0, 1, \ldots, G.$$

This procedure is easily implemented by constructing a Diagonal-Look-Up-Table (DLUT) from the composition matrix $Q(O)$. For each k'_0, the diagonal hanging to the right is taken, and its maximum element determined. The corresponding k value is assigned to the entry k'_0 in the LUT.

Fig. 4 shows the comparative results of filtering Lena with 30% salt & pepper noise. Since no training set of images are defined for the class of Lena, a theoretical model (the hypergeometrical one) has been used as default. The result for the Model Restoration filter is the only one that removes all the noise.

4. Results and discussion

Besides the examples given above to illustrate the proposed filters, more complete experimental results for the same original images are presented now, along with some general comments. Experiments have been carried out under the following settings:

1. **Sliding window**. A square window is always used, the size being either 3×3 or 5×5.
2. **Image scanning and grey scale**. All images have been captured by scanning with 8-bits grey scale, all using the same settings. They were stored in TIFF, and then the grey scale was linearly reduced to 6 bits (0–63) for easier handling.
3. **Quality measures**. Although visual estimation remains the main way to assess the enhancement results, a more reliable comparative study of our filters would require a quantitative measure. From those proposed and used [14], the mean absolute error $\text{MAE} = \Sigma|I_1 - I_2|/(V \times H)$ was chosen, I_1 and I_2 being the images to be compared, and $V \times H$ being their common size.
4. **Iterations**. As frequently happens, the filtered image improves through successive passes of the filter algorithm. The results offered here correspond to five iterations, unless indicated. It should be borne in mind that the iteration in the filtering passes implies that some modification must be made in the used mask.

Numerical results are summarized in Table 4.

4.1. Discussion

Mask-Model filters have proven to be much better than those used for comparison. The MAE reduction reaches up to nine times. The conventional median and the weighted-median filters work better than the new filters in only one case throughout the table, namely for a radiograph strongly corrupted with G-noise. Nevertheless, visual results are very close in this case (see Fig. 1).

The numerical results for a given source are very similar, in general, for the different filters used. However, the following remarks are in order:

1. It can be said that the mask-matrix filter has revealed itself as surprisingly good, bearing in mind that one the mask has been obtained, the filter pass takes into account only the whole-window grey level. This emphasizes the strong role played by the mask.
2. Some cases are favorable for the mask-model weighted filter. This filter has been designed to mutually reinforce the fairly good quality of the mask-median and the mask-matrix. However, although truly comparable, the results are better in only a few cases, such as in the echograph corrupted with dense noise.

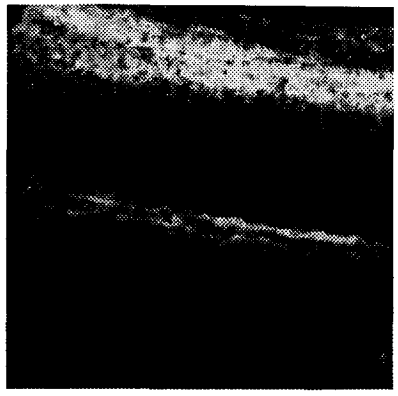

Original

Source
(20% uniformly distributed noise)

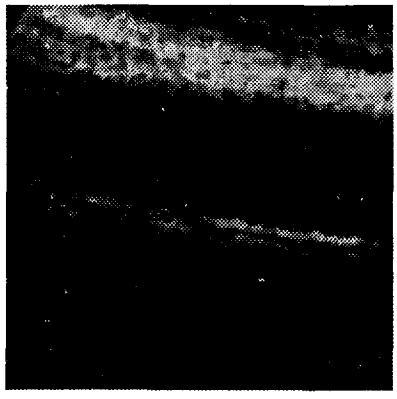

3 × 3 Median Filter

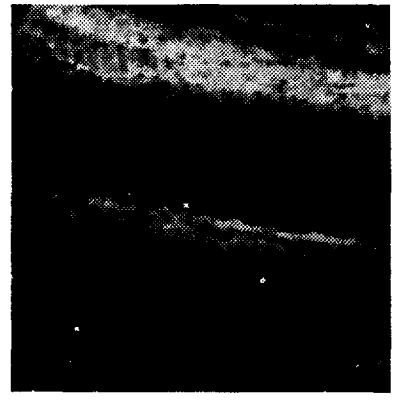

3 × 3 Central Weighted Median Filter

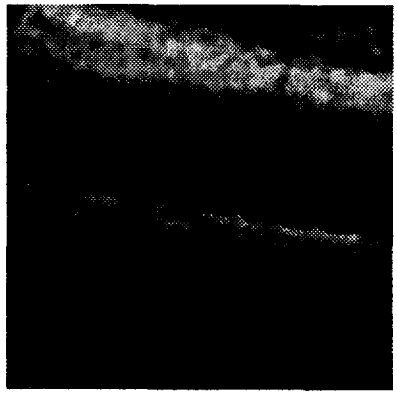

Adaptive Filter
(Sun & Venetsanopoulos)

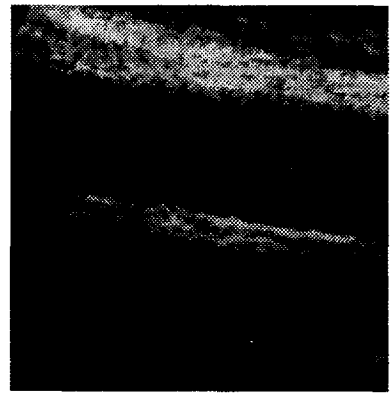

3 × 3 Mask-Model Weighted Filter
(selection ratio $\rho = 10\%$)

Fig. 3. Median and central weighted median filtering, Sun & Venetsanopoulos' adaptive filtering and mask-model weighted filtering example for a echograph image. (a) Original, (b) source (20% uniformly distributed noise), (c) 3 × 3 Median filter, (d) 3 × 3 Central Weighted Median filter, (e) Adaptive filter (Sun & Venetsanopoulos), (f) 3 × 3 Mask-Model Weighted filter (selection ratio $\rho = 10\%$).

Original

Source
(30% salt & pepper noise)

3 × 3 Median Filter

3 × 3 Central Weighted Median Filter

Adaptive Filter
(Sun & Venetsanopoulos)

3 × 3 Model Restoration Filter
(selection ratio $\rho = 0\%$)

Fig. 4. Median and central weighted median filtering, Sun & Venetsanopoulos' adaptive filtering and model-restoration filtering example for Lenna. (a) Original, (b) source (30% salt & pepper noise), (c) 3 × 3 Median filter, (d) 3 × 3 Central Weighted Median filter, (e) Adaptive filter (Sun & Venetsanopoulos), (f) 3 × 3 Model Restoration filter (selection ratio $\rho = 0\%$).

3. Very good results can be obtained for the restoration-model filter, the only one differently designed. Its best performance in filtering Lenna deserves particular interest, since a theoretical model has been used.

4.2. Remarks and properties

1. **Low noise**. For low noise levels, these four median-type filters are more advantageous than others. This is because the main rationale is not to filter the good pixels. Thus, a noise-free, good-model image is probably a root.
2. **Roots**. The problem of finding the roots [14] in the mask-median filter is complex, and depends on the composition matrix. However, it is strongly simplified for the assumption of an ideal mask $\tilde{M} = M$, whatever the model may be. Then the non-filtered subimage is clearly a subroot, while the complementary subimage is median-filtered, thus having the same root behavior as the conventional median filter. Roughly speaking, the mask-median filter has the root properties of the median filter, but with an expected faster convergence. This is fully achieved, as can be checked throughout Table 1.
3. **Stacking**. Because of the composition model, these filters do not have the threshold decomposition property, thus they are not stack filters. If so, a set of binary (two-row) composition matrices would have to be derived, one for each stack level. However, this set would either represent an inconsistent model, or be a universal model, independent of the class of images.
4. **Blotches**. The known, undesirable property of the median-type filters of generating patches or blotches as an artifact of the procedure, is attenuated in the mask-median filter. Pitas [3] discusses this, and proposes a measurement of the blotch effect by means of the probability of giving the same output for two pixels, under certain assumption, as a function of the distance between them. These or any other analyses are applicable to the filtered pixels in the Mask-Model filters, but the difference is that not all the pixels are filtered. Any measurement valid for two pixels in the median filter should be reduced by the probability of these two pixels to be filtered, as a factor. This probability is calculated in a straightforward manner under the simplifying assumption $\tilde{M} = M$. Since the impulsive noise is spatially independent, if p is the probability of filtering a given pixel, the probability for two is p^2. This is, therefore, the approximate

Table 4
Experimental results for comparing the new Mask-Model filters with three known ones as reference and four classes of images. Best results are in bold. The ! symbol means that the filter did not converge after five iterations, so the MAE could decrease even more; the + sign means the filter gave the best result after the fifth iteration and then MAE increases until convergence. § w/n/s: $w \times w$ window size/kind of noise (sp = salt & pepper; g = uniformly distributed) n% of noise/s% of selection ratio

Config§	MAE (S-O)	median MAE	wei-med MAE	ada-sun MAE	mod-rest MAE	mask-med MAE	mod-wei MAE	mask-matrix MAE
Radiograph								
3/SP10/0	3.11	0.11	0.08	0.23	**0.0201**	0.0207	0.021	0.0207
5/SP10/0	3.11	0.15	0.11	0.23	0.019	**0.018**	0.019	0.02
3/SP20/0	6.31	0.13	0.16	0.43	**0.0401**	0.043	0.042	0.0404
5/SP20/0	6.31	0.16	0.12	0.43	0.044	**0.043**	0.044	0.045
3/SP30/0	9.56	0.15	0.35	0.59	**0.064**	0.068	0.068	0.065
5/SP30/0	9.56	0.18	0.16	0.59	0.088	**0.087**	0.088	0.089
3/G10/1	2.75	0.12	0.09	0.01	0.030	**0.027**	0.031	0.030
5/G10/1	2.75	0.15	0.11	1.01	0.025	**0.023**	0.024	0.026
3/G20/1	5.47	0.16	0.24	3.09	0.14	**0.10**	0.15	0.14
5/G20/1	5.47	0.20	0.15	3.09	0.084	**0.082**	0.083	0.085
3/G30/1	8.06	**0.23**	0.76	5.76	0.418	0.298	0.457	0.422
5/G30/1	8.06	0.25	**0.20**	5.76	1.254	1.218	1.278	1.257
Text								
5/0/0	0.00	3.31	2.19	1.63	0.0029	**0.0028**	0.0029	0.0029
3/SP10/0	3.18	1.77	1.03	2.07	0.35	0.25	0.29	**0.24**
5/SP10/0	3.18	3.31	2.28	2.07	0.49	**0.39**	0.45	0.40
3/SP20/0	6.29	2.09	1.56	2.65	0.67	0.50	0.56	**0.47**
5/SP20/0	6.29	3.37	2.41	2.65	0.89	**0.71**	0.82	0.73
3/SP30/0	9.28	2.48	2.06	3.34	1.01	0.81	0.87	**0.75**
5/SP30/0	9.28	3.44	2.59	3.34	1.34	**1.08**	1.27	1.12
3/G10/1	2.57	1.78	1.06	3.00	0.88	0.68	0.80	**0.66**
5/G10/1	2.57	3.28	2.31	3.00	0.71	**0.66**	0.69	0.67
3/G20/1	5.10	2.19	1.70	5.04	1.43	1.26	1.42	**1.24**
5/G20/1	5.10	3.34	2.49	5.04	1.603	**1.396**	1.551	1.405
3/G30/1	7.59	2.76	2.48	7.32	2.53	2.56	2.70	**2.43**
5/G30/1	7.59	3.54	2.96	7.32	2.29	**2.05**	2.21	2.09

reduction factor of the blotch effect. The reduction may be observed in the filtered text image in Fig. 2.

5. **Robustness**. As a measure of the robustness, the breakpoint has been defined as the number of aberrant pixels in the window that cause the output to be aberrant [15]. This measurement is difficult to calculate because of the inherent statistic. However, the breakpoint is easy to estimate if $\tilde{M} = M$ is assumed again, since an ideal mask detects all aberrant pixels for filtering, and neither of them in the window is used for substituting a bad pixel. The only possible aberrant output happens when all pixels in the window are aberrants, since the filter cannot proceed. In this case the breakpoint is 100%. The robustness of these filters can be visually observed in Figs. 1–4.

4.3. Influence of the filter parameters

1. **The window**. The four proposed filters work better with windows of 3×3 than 5×5, with respect to the results of the other filters. However, the difference decreases as the noise increases. Obviously, the larger the window, the fewer the details detected.
2. **The noise**. The general behavior with respect to the noise is highlighted in the noise-free experiment shown in the first row in Table 1 (text). The MAE

Table 4 Continued

Config[§]	MAE (S-O)	median MAE	wei-med MAE	ada-sun MAE	mod-rest MAE	mask-med MAE	mod-wei MAE	mask-matrix MAE
Echograph								
3/SP10/0	3.24	0.52	0.32	0.93	0.070	0.0725	0.0716	**0.0677**
5/SP10/0	3.24	0.85	0.61	0.93	0.113	**0.097**	0.0988	0.104
3/SP20/0	6.26	0.63	0.46	1.22	0.141	0.147	0.143	**0.135**
5/SP20/0	6.26	0.89	0.66	1.22	0.223	**0.193**	0.197	0.205
3/SP30/0	9.56	0.74	0.74	1.60	0.225	0.250	0.240	**0.222**
5/SP30/0	9.56	0.95	0.73	1.60	0.336	**0.303**	**0.303**	0.313
3/G10/1	2.27	0.51	0.31	1.38	0.127	0.128	0.126	**0.125**
3/G10/5	2.27	0.51	0.31	1.38	0.096	0.098	0.095	**0.094**
3/G10/10	2.27	0.51	0.31	1.38	0.100	0.100	0.0989	**0.0977**
5/G10/1	2.27	0.85	0.61	1.38	0.18	**0.17**	0.171	0.175
5/G10/5	2.27	0.85	0.61	1.38	0.163	**0.151**	0.154	0.157
5/G10/10	2.27	0.85	0.61	1.38	0.201	**0.184**	0.187	0.191
3/G20/1	4.68	0.68	0.53	3.08	0.256	0.256	0.255	**0.254**
3/G20/5	4.68	0.68	0.53	3.08	0.207	0.209	0.207	**0.205**
3/G20/10	4.68	0.68	0.53	3.08	0.211	0.208	**0.207**	**0.207**
5/G20/1	4.68	0.931	0.69	3.08	0.346	**0.326**	0.329	!0.334
5/G20/5	4.68	0.931	0.69	3.08	0.302	**0.28**	0.283	0.289
5/G20/10	4.68	0.931	0.69	3.08	0.328	**0.304**	0.309	0.313
3/G30/1	7.12	0.934	0.99	5.21	0.461	**!0.445**	0.449	0.459
3/G30/5	7.12	0.934	0.99	5.21	0.497	**!0.428**	!0.446	0.472
3/G30/10	7.12	0.934	0.99	5.21	0.497	**!0.434**	!0.453	0.489
5/G30/1	7.12	1.12	0.89	5.21	0.535	**0.502**	0.504	0.520
5/G30/5	7.12	1.12	0.89	5.21	0.461	**0.425**	0.428	0.440
5/G30/10	7.12	1.12	0.89	5.21	0.462	**0.428**	0.432	0.442
Lenna								
3/SP10/0	12.66	2.35	1.51	4.69	**0.747**	!0.765	!0.770	**+0.747**
3/SP20/0	22.58	2.74	2.23	6.85	**1.091**	!1.144	!1.149	**+1.091**
3/SP30/0	38.17	3.19	3.42	9.18	**1.429**	!1.525	!1.533	**+1.429**
3/G10/0.1	7.05	2.38	1.48	4.50	**0.897**	!0.909	!0.914	**+0.897**
3/G10/0.5	7.05	2.38	1.48	4.50	1.029	!1.05	!1.058	**+1.028**
3/G10/1	7.05	2.38	1.48	4.50	1.029	!1.052	!1.058	**+1.028**
3/G10/5	7.05	2.38	1.48	4.50	**1.310**	!1.34	!1.349	**+1.310**
3/G10/10	7.05	2.38	1.48	4.50	**1.509**	!1.56	!1.563	**+1.509**
3/G20/0.1	14.21	2.84	2.21	7.18	**+1.450**	!1.469	!1.475	+1.453
3/G20/0.5	14.21	2.84	2.21	7.18	**+1.518**	!1.549	!1.554	+1.519
3/G20/1	14.21	2.84	2.21	7.18	**+1.518**	!1.549	!1.554	+1.519
3/G20/5	14.21	2.84	2.21	7.18	**+1.706**	!1.766	!1.761	+1.707
3/G20/10	14.21	2.84	2.21	7.18	**+1.905**	!1.971	!1.970	+1.905
3/G30/0.1	21.4	3.33	3.06	10.52	**2.080**	!2.088	!2.099	2.081
3/G30/0.5	21.4	3.33	3.06	10.52	**2.103**	!2.128	!2.141	2.114
3/G30/1	21.4	3.33	3.06	10.52	**2.103**	!2.128	!2.141	2.114
3/G30/5	21.4	3.33	3.06	10.52	**+2.288**	!2.322	!2.340	+2.290
3/G30/10	21.4	3.33	3.06	10.52	**+2.440**	!2.484	!2.491	+2.442

shows the improvement compared to other filters. In Mask-Model filters, only a few pixels (16) have been processed, against the high number of pixels (40,000) in the image. This number shows the success of Mask-Model filters.

3. **The selection factor**. The more the cohesion in a model, the more its reliability, in the sense that the grey levels the model considers as probable prove to be possible in reality. On the other hand, a low-cohesion model may assign some probability to grey levels that actually never appear in any window. Thus, the less cohesion a model has, the higher a selection ratio ρ must be chosen, because the aim is to recognize the noise.
4. **The model**. Very subtle, local differences can be appreciated with respect to the model used. As an example, the radiograph is better filtered (with respect to the reference filters again) than other images. The theoretical analysis needs a more complex study of the model quality in relation to the operations involved in masking and filtering.
5. **Iterations**. Only the results obtained with the Lena image show different convergence behavior, depending on the filter, because the hypergeometric model is not the ad hoc one for Lena. Model-restoration and mask-matrix filters reach the root because their operation is more determined by the model.

5. Conclusions

Four new variants of the median-type filter, called Mask-Model filters, have been developed with the aim of reducing the usual damaging side-effects due to the processing of the good, non-corrupted pixels in the image. This is achieved by means of a noise-estimation mask, which preselects the pixels that must be processed. The mask is obtained from the information provided beforehand by a suitable composition model. The behavior of these filters has been examined with respect to the different configuration operations.

The results have proven these new filters to be must more efficient in removing impulsive noise than the other known median-type filters. Also, they show good root-finding, blotch effect and robustness, although they are not stack filters. Theoretical analyses of the performance and properties of the filters are currently being investigated by the authors, as well as the promising application of these filters in cases where the empirical model is available with a good enough quality.

Acknowledgement

This work was supported in part by Grant TIC91-0646 from the Spanish Government.

References

[1] H.A. Davis, Order Statistics, John Wiley, Chichester, 1980.
[2] P.S. Huber, Robust Statistics, John Wiley, Chichester, 1981.
[3] I. Pitas and A.N. Venetsanopoulos, Nonlinear Digital Filters: Principles and Applications, Kluwer Academic, Netherlands, 1990.
[4] B.I. Justunsson, Median filtering: statistical properties, in Two Dimensional Digital Signal Processing II, T.S. Huang (ed.), Springer-Verlag, Berlin, 1981.
[5] P.D. Wendt, E.J. Coyle and N.C. Gallagher Jr., Stack filters, IEEE Trans. Acopust. Speech and Signal Proc., 34(4) (August 1986) 898–911.
[6] R. Román-Roldán, J.J. Quesada-Molina and J. Martínez-Aroza, Multiresolution-information analysis for images, Signal Processing, 24 (July 1991) 77–91.
[7] L. García-Cabrera, P.L. Luque-Escamilla, J. Martínez-Aroza, A.M. Robles-Pérez and R.T. Román-Roldán, Some pixel-preselection methods for median-type filtering, in preparation.
[8] J. Martínez-Aroza and R. Román-Roldán, Probabilistic linear models for grey-level image estimation, Multidim. Syst. Sign. Proc., 6 (1995) 7–35.
[9] R. Román-Roldán, J. Martínez-Aroza, M.J. García-Salinas, P.L. Luque-Escamilla and J.C. Segura-Luna, Multiresolution empirical models for grey-level images, in preparation.
[10] J. Lin, Divergence measures based on the Shannon entropy, IEE Trans. Inf. Theory, 37(1) (1991) 145–150.
[11] X.Z. Sun and A.N. Venetsanopoulos, Adaptive schemes for noise filtering and edge detection by use of local statistics, IEEE Trans. Circuits and Systems, 35(1) (January 1988) 57–70.
[12] G.R. Arce and R.E. Foster, Detail-preserving ranked-order based filters for image processing, IEEE Trans. Acopust. Speech and Signal Proc., 37(1) (January 1989) 83–98.
[13] A. Nieminen, P. Heinonen and Y. Neuvo, A new class of detail-preserving filters for image processing, IEEE Trans. Pattern Anal. Machine Intell., 9(1) (January 1987) 74–90.
[14] E.J. Coyle, J.H. Lin and M. Galdbouj, Optimal stack filtering and the estimation and structural approaches to image processing, IEEE Trans. Acoust. Speech and Signal Proc., 37(12) (1989) 2037–2066.
[15] H. Longbotham and D. Eberly, Statistical properties, fixed points and decomposition with WMMR filters, J. Math. Imaging and Vision, 2 (1992) 99–116.